Negative refraction via radiative surface phonon polaritons in a silicon carbide–based multilayer structure

Olalekan Adewuyi
James S. Hammonds, Jr.

Negative refraction via radiative surface phonon polaritons in a silicon carbide–based multilayer structure

Olalekan Adewuyi and James S. Hammonds, Jr.
Howard University, Mechanical Engineering Department,
Washington, District of Columbia 20059
E-mail: j_hammonds@howard.edu

Abstract. In this letter, we predict that radiative surface phonon polariton (RSPhP) modes, in a multilayer structure consisting of thin-film silicon carbide (SiC) bounded by silicon (Si) and diamond (Di), can be used to achieve negative refraction of mid-infrared light at approximately 11 μm. Dispersion relations, calculated for the Si/SiC/Di structure, show that the RSPhP mode exhibits negative dispersion and couples with incident light. Poynting vector calculations show how the energy flux may be refracted, negatively, in the SiC layer. © 2012 Society of Photo-Optical Instrumentation Engineers.

Currently, there is great interest in materials that refract light negatively. Negative refraction can be characterized by a light beam whose wavefront is refracted normally (in a positive direction), while its energy flux is refracted negatively. Materials that negatively refract light can enable applications such as near-field superlensing and optical cloaking.[1] Approaches to developing negative refraction materials include the design of photonic crystals with geometries that result in desired dispersion properties. The photonic crystal approach has produced some notable successes in the development of microwave to infrared negative refraction materials.[2,3] Another approach is to exploit material resonance modes to achieve negative refraction.[4,5] Recent examples include the use of infrared plasma resonance in free-carrier doped InGaAs films to suport negative refraction.[6] Magnetic resonance, in gold, has also been applied to the development of mid-IR negative refraction materials.[7] In this letter, we propose that coupled photon-phonon resonance modes, called radiative surface phonon polaritons (RSPhP), can be exploited in the development of mid-IR negative refraction materials. To demonstrate this idea, we present theoretical results for a prototype structure consisting of a thin silicon carbide (SiC) film, bounded by very thick layers of silicon (Si) and diamond (Di). Approaches to achieving mid-IR negative refraction materials are necessary for the development of next-generation thermal management devices such as thermal rectifiers and specialized thermal emitters.[8,9]
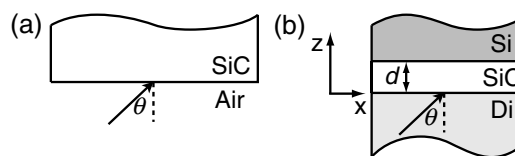

Fig. 1 (a) Schematic of semi-infinite SiC/Air system. (b) Schematic of Si/SiC/Di structure studied in this work, where d is the SiC thickness, and θ is the angle of the incident light.

Physically, surface phonon polaritons are atomic lattice-waves coupled to transverse magnetic (p-polarized) electromagnetic fields that may be supported at the interface between a polar material bounded by a dielectric. For example, surface phonon polaritons can be excited at the interface between air (dielectric constant, $\epsilon_0 \approx 1$) and a semi-infinite layer of SiC [a polar material with a frequency varying dielectric function $\epsilon_1(\omega)$]. The SiC/Air system is illustrated in Fig. 1(a), and the well-known dispersion relation for surface phonon polariton modes at an interface formed between a semi-infinite polar material and a dielectric is given by the expression

$$k_x = \frac{\omega}{c} \sqrt{\frac{\epsilon_0 \epsilon_1(\omega)}{\epsilon_0 + \epsilon_1(\omega)}}, \qquad (1)$$

where the dependency on frequency ω is made explicit and where c is the speed of light. The surface phonon polariton dispersion relation for the SiC/Air case is plotted as the dotted line in Fig. 2. The vertical axis of Fig. 2 is the frequency at which the surface mode exists and the horizontal axis is (the real part of) k_x, which is the wavevector for the surface polariton that is propagating parallel to the SiC interface. The "light line" is the dashed diagonal line through the plot and gives the dispersion relation for light propagation in free space, or $k = \omega/c$. The upper and lower limits of the frequency axis, in Fig. 2, approximately correspond to the spectral locations of the SiC transverse optical frequency ω_{TO} and its longitudinal optical frequency ω_{LO}, which gives the SiC/Air polariton dispersion cutoff. Between these
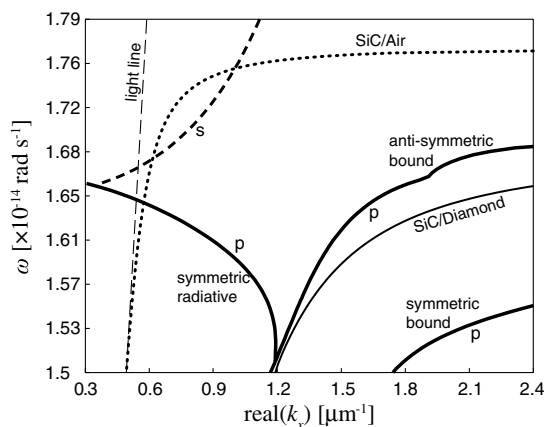

Fig. 2 Frequency versus the real part of k_x. Thin Dashed Line: Free space light line. Dotted Line: SPhP dispersion relation for semi-infinite SiC bounded by air [Fig. 1(a)]. Solid Thick Lines: SPhP dispersion relation for p-polarized light in multilayer structure shown in Fig. 1(b). Thick Dashed Line: Dispersion relation for s-polarized light in the multilayer structure. Thin Solid Line: Dispersion relation for semi-infinite SiC bounded by diamond.

frequency limits, the dielectric function of SiC is less than zero, i.e. $\epsilon_1(\omega) < 0$, and a negative dielectric indicates that the material may support electromagnetic resonance modes. More specifically, the SiC dielectric function can be described by the Lorentz model $\epsilon_{SiC}(\omega) = \epsilon_\infty(\omega_{LO}^2 - \omega^2 - i\gamma\omega)/(\omega_{TO}^2 - \omega^2 - i\gamma\omega)$ where $\epsilon_\infty = 6.7$, $\omega_{LO} = 18.3 \times 10^{13}$ s^{-1}, $\omega_{TO} = 14.9 \times 10^{13}$ s^{-1}, and the damping constant is given as $\gamma = 0.89 \times 10^{12}$ s^{-1}. In this letter, the loss term γ is included in all calculations.

The wavevector representing the component of light propagating perpendicular to i'th interface is defined by $k_{zi} = \sqrt{\epsilon_i k^2 - k_x^2}$. Therefore, surface modes with $k_x > \epsilon_i k$ cannot couple to propagating light, since k_{zi} would be purely imaginary. Figure 2 shows that the surface phonon polariton mode for the SiC/Air structure is to the right of the light line and, thus, k_x is too large for a beam of incident light to interact with the surface phonon polariton.

So, while it is possible for semi-infinite SiC to support mid-IR surface phonon polaritons, these modes are forbidden from direct coupling to propagating light. However, the situation completely changes for the case of a thin, 400 nm layer of SiC, sandwiched between semi-infinite thick layers of Si and diamond, as shown in Fig. 1(b). These materials were chosen because they are transparent in the infrared region and have high refractive indexes with $n_{Si} = 3.5$ and $n_{Di} = 2.4$. The dispersion relation, for surface phonon polaritons in the Si/SiC/Di structure, is determined by numerically finding values of $k_x(\omega)$ that result in zeros for the denominator of the three-layer, p-polarized, reflectance equation,[10]

$$R_{210}^p = \left| \frac{r_{21}^p + r_{10}^p e^{2i\alpha_1}}{1 + r_{21}^p r_{10}^p e^{2i\alpha_1}} \right|^2, \qquad (2)$$

where

$$r_{ij}^p = \left(\frac{k_{zi}}{\epsilon_i} - \frac{k_{zj}}{\epsilon_j} \right) \Big/ \left(\frac{k_{zi}}{\epsilon_i} + \frac{k_{zj}}{\epsilon_j} \right), \qquad (3)$$

$\alpha_1 = k_{z1}d$, and the subscripts refer to the layers $i, j = 0, 1$, and 2, where diamond is layer 0, SiC is layer 1, and Si is layer 3. The numerically determined surface phonon polariton dispersion relation for the Si/SiC/Di structure is given by the solid thick lines of Fig. 2, and shows three branches. Two branches are completely to the right of the light line and represent modes unaccessible by propagating light. As shown in the figure, the two modes are the antisymmetric and symmetric modes which are well-known to represent the surface polaritons at each interface the thin film.[10] The plot also shows the dispersion relation for semi-infinite SiC bounded by diamond. While the horizontal axis range is limited in Fig. 2 for brevity, previous theoretical results suggest that for very large k_x, degeneracy is lifted and the symmetric and anti-symmetric modes become equivalent to the semi-infinite SiC/Diamond case. The SPhP modes are known to only exist for the p-polarized case. For comparison, we also plot the dispersion relation for the s-polarized case in Fig. 2 to show that the effects discussed in this letter only occur for p-polarized light.

The third branch of the Si/SiC/Di dispersion relation extends to the left of the light line, crossing it at approximately $\omega = 1.65 \times 10^{14}$ rad s^{-1}, or 11.4 μm. Since this mode crosses the light line and is, thus, accessible by propagating

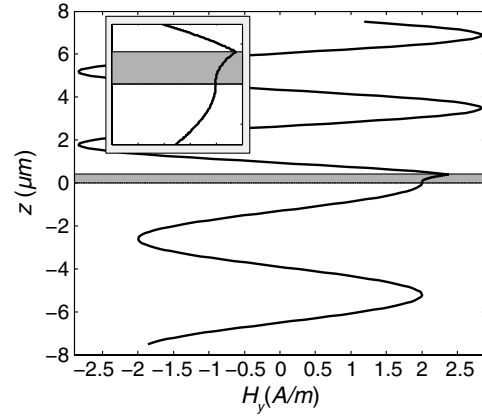**Fig. 3** Magnetic field distribution in three layer structure at 11.4 μm. Inset: Details of magnetic field inside SiC layer.

light with a wavelength of about 11.4 μm, we refer to it as a radiative surface phonon polariton (RSPhP). As will be shown below, calculation of the magnetic field shows that the mode is symmetric since the transverse component of the electric field (E_z) is not zero inside the film [c.f. Fig. 3 and Eq. (4)]. Symmetric (and anti-symmetric) radiative surface polaritons have been predicted, before, for the case of multilayer structures. However, our calculations show that the radiative branch of the dispersion relation presented here has a negative slope. Since the group velocity is given by $v_g = \partial\omega/\partial k$, the negative slope implies a negative group velocity. Also, since the group velocity characterizes the direction of energy flow, which in this case is roughly opposite of the wave propagation direction (k_x), negative refraction may be possible with the structure shown in Fig. 1(a). To validate that the radiative mode is a physical solution, we calculated the imaginary part of k_x for the RSPhP mode as positive. Thus, the surface mode decays as it propagates along the film, radiating light into the silicon along the way.

In the remainder of this letter, we will use theoretical evidence to support the idea that incident light coupling to radiative surface phonon polariton modes can be accomplished in the Si/SiC/Di structure. We also use theoretical results to show that negative refraction is occurring in the SiC layer of the Si/SiC/Di structure. We can characterize this light coupling by examining the magnetic field in the Si/SiC/Di structure. Referring to the system shown in Fig. 1(b), we start by describing the magnetic field in each layer as

$$H_{y2} = e^{i(k_x x - \omega t)} e^{-k_{z2}z} \qquad z \geq d, \qquad (4)$$

$$H_{y1} = e^{i(k_x x - \omega t)}(Ae^{k_{z1}z} + Be^{-k_{z1}z}) \qquad 0 \leq z \leq d, \qquad (5)$$

$$H_{y0} = Ce^{i(k_x x - \omega t)} e^{-k_{z0}z} \qquad z \leq 0. \qquad (6)$$

The boundary conditions require that the magnetic fields and their derivatives be continuous at each interface, e.g., $H_{y0} = H_{y1}$, and $(1/\epsilon_1)(\partial H_{y1}/\partial z) = (1/\epsilon_2)(\partial H_{y2}/\partial z)$ at $z = 0$. By manipulating Eqs. (4) through (6) and applying the attendant boundary conditions, we find

$$A = \left[\frac{\epsilon_1 k_{z0}}{\epsilon_0 k_{z1}} + 1 \right], \quad B = \left[\frac{\epsilon_1 k_{z0}}{\epsilon_0 k_{z1}} - 1 \right], \quad \text{and} \quad C = A + B. \qquad (7)$$

The magnetic field is plotted for the case of 11.4 μm light in Fig. 3, where the gray region represents the SiC layer.

Figure 3 shows the infrared light propagating through the diamond layer as an oscillating field below the gray region. The gray region is the SiC layer. Figure 3 also shows the field exponentially decaying within the SiC layer, which is characteristic of a surface phonon polariton mode. The inset of Fig. 3 shows the details of the exponential decay in the SiC layer. Finally, another oscillating field is shown in the region above the SiC region, which demonstrates that the RSPhP mode is leaking into the silicon layer. Furthermore, the results show that the RSPhP mode is not self-sustaining, but depends on infrared light incident from the diamond side.[11]

We now, theoretically, show that the 11.4 μm light energy flux is negatively refracted in the Si/SiC/Di structure. The Poynting vector describes the light energy flux as

$$\mathbf{S} = \mathbf{E} \times \mathbf{H} = (-H_y E_z)i + (H_y E_x)\mathbf{k}, \tag{8}$$

and thus the direction of the energy flux in the material is given by

$$\tan\theta = -\frac{E_x H_y}{H_y E_z}, \tag{9}$$

where the magnetic fields are given by Eqs. (4) through (6), and Maxwell's equations give the associated electric fields as

$$E_{xi} = -\frac{ic}{\omega\epsilon_i}\frac{\partial H_{yi}}{\partial z} \quad \text{and} \quad E_{zi} = -\frac{k_x c}{\omega\epsilon_i} H_{yi}, \tag{10}$$

which when used with Eq. (9) for each layer, we obtain

$$\tan\theta = -\frac{ik_{z2}}{k_x} \qquad z > d, \tag{11}$$

$$\tan\theta = -\frac{ik_{z1}(Be^{k_{z1}z} - Ce^{-k_{z1}z})}{k_x(Be^{k_{z1}z} + Ce^{-k_{z1}z})} \qquad 0 < z < d, \tag{12}$$

$$\tan\theta = -\frac{ik_{z0}}{k_x} \qquad z < d. \tag{13}$$

The energy flux directions for p-polarized 11.4 μm light in Si/SiC/Di is plotted in Fig. 4.

Figure 4 shows that the energy flux has a positive incidence angle at the SiC/Di interface which we calculate from Eq. (11) to be $\theta_0 = 66$ deg. The energy flux then, dramatically, changes its angular direction in the SiC such that it is negatively refracted as it propagates from the diamond to the Si/SiC interface. The flux angle in the SiC layer, θ_1, is calculated using Eq. (12). The real part of θ_1 varys from -80 deg to -73 deg, and is plotted in Fig. 4. The curvature of the energy flux in the SiC layer is consistent with Fermat's
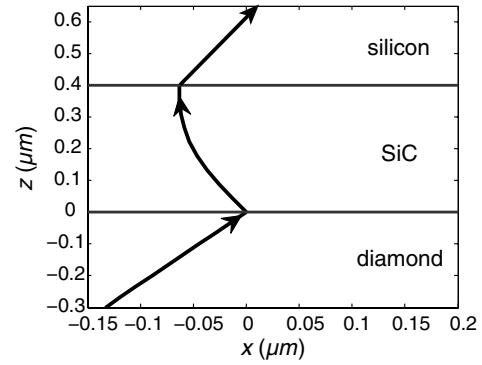

Fig. 4 Energy flux direction of 11.4 μm mode in each layer of the Si/SiC/Di structure.

principle, since there is significant variation in refractive index from the diamond to Si layers. The energy flux emerges from the SiC/Si interface again with a positive angle calculated, with Eq. (13), to be $\theta_2 = 74$ deg.

In conclusion, this letter, theoretically, predicts that a submicron thin film of SiC, bounded by silicon and diamond, may be used as a negative refraction material. The key mechanism is the radiative surface phonon polariton mode coupled to incident light at the SiC interfaces.

References

1. S. Kawata, Y. Inouye, and P. Verma, "Plasmonics for near-field nano-imaging and superlensing," *Nat. Photonics* **3**(7), 388–394 (2009).
2. A. Berrier et al., "Negative refraction at infrared wavelengths in a two-dimensional photonic crystal," *Phys. Rev. Lett.* **93**(7), 73902 (2004).
3. E. Schonbrun et al., "Wave front evolution of negatively refracted waves in a photonic crystal," *Appl. Phys. Lett.* **90**(4), 041113 (2007).
4. J. Yao et al., "Optical negative refraction in bulk metamaterials of nanowires," *Science* **321**(5891), 930–930 (2008).
5. V. Shalaev, "Optical negative-index metamaterials," *Nat. photonics* **1**(1), 41–48 (2007).
6. A. Hoffman et al., "Negative refraction in semiconductor metamaterials," *Nat. Mater.* **6**(12), 946–950 (2007).
7. J. Bossard et al., "Synthesizing low loss negative index metamaterial stacks for the mid-infrared using genetic algorithms," *Opt. Express* **17**(17), 14771–14779 (2009).
8. S. Basu and M. Francoeur, "Near-field radiative transfer based thermal rectification using doped silicon," *Appl. Phys. Lett.* **98**(11) 113106 (2011).
9. C. Fu and Z. Zhang, "Further investigation of coherent thermal emission from single negative materials," *Nanoscale Microsc. Thermophys. Eng.* **12**(1), 83–97 (2008).
10. H. Raether, *Surface Plasmons on Smooth and Rough Surfaces and on Gratings*, Springer, Berlin (1988).
11. J. Burke, G. Stegeman, and T. Tamir, "Surface-polariton-like waves guided by thin, lossy metal films," *Phys. Rev. B* **33**(8), 5186 (1986).

Biographies and photograph of the authors are not available.